

# Numerical Study of Optical Injection Dynamics of Vertical-Cavity Surface-Emitting Lasers

M. S. Torre, Cristina Masoller, and K. A. Shore

**Abstract**—We study numerically the transverse-mode dynamics of a vertical-cavity surface-emitting laser with external optical injection. We consider the case in which two transverse modes with parallel polarizations are excited. Varying the strength and frequency of the injected field, we find a rich variety of complex behaviors. We show that by increasing the optical injection strength the laser does not turn into a single-mode laser, as would be expected if the transverse modes have perpendicular polarizations.

**Index Terms**—Antiphase dynamics, chaotic oscillations, injection locking, optical injection, vertical-cavity surface-emitting lasers (VCSELs).

## I. INTRODUCTION

VERTICAL-CAVITY SURFACE-EMITTING LASERS (VCSELs) are promising devices for applications that require stable single-mode operation under high-speed modulation. Injection locking of a slave laser to a master laser is a technique commonly employed to enhance the spectral stability and to minimize the chirping of lasers. In VCSELs, the influence of optical injection from an edge-emitting laser or from another VCSEL was studied theoretically and experimentally by several authors [1]–[10]. It has been shown that the polarization state of a VCSEL can be switched by optical injection [1]. Stable phase locking within a large detuning range has been reported, as well as a variety of nonlinear behaviors outside the locking range [2]. In [3], it was shown that the bistability inherent to polarization locking allows for generating a memory effect by modulating the bias current of the master laser. In [4], the polarization state of the light emitted by a slave VCSEL was controlled by injecting an orthogonally polarized optical signal from a master VCSEL. By modulating the bias current of the master VCSEL, fast polarization switching in the slave VCSEL was observed. Phase tuning of two slave VCSELs, being injection-locked by a master VCSEL, was demonstrated in [5]. Injection-locking by injected optical power from another VCSEL improves the transmission performance of a directly modulated VCSEL [6]. Optical injection was also found to induce chaos and dynamic instability [7], [8] in the polarization-resolved output power of

a VCSEL operating, without injection, in a stable polarization regime.

The short cavity length of VCSELs ensures single longitudinal mode operation, but due to their large Fresnel number high-order transverse modes are easily excited. Li *et al.* [2] observed that, when the master laser frequency was detuned to be coincident with the frequency of one transverse mode of the slave VCSEL, this mode was enhanced and the other mode was partially or even totally suppressed. Based on a model that included the spatial dependence of the carrier density and of the optical field, Law *et al.* [9] showed that a two-transverse-mode VCSEL could be forced, due to optical injection, to operate in a single transverse mode. It was assumed that the two transverse modes had orthogonal polarizations, and thus the externally injected field interfered only with one of the modes. More recently, Hong *et al.* [10] studied experimentally the spectrum of a two-transverse-mode VCSEL under optical injection and found that, in agreement with the results of [2] and [9], when the two modes have orthogonal polarizations, suitably choosing the detuning and injection power allows the suppression of one mode. However, it was found that when the two transverse modes have parallel polarization single-mode operation could not be obtained via optical injection. In this paper, we use a model similar to that employed by Law *et al.* [9] to understand the behavior of an optically injected VCSEL having two transverse modes with parallel polarization. In simpler models where, e.g., spatial effects are omitted, quite complex optical injection dynamics may arise [17]–[25]. As such, it is to be expected that the model used in this work will yield a range of instabilities and various dynamical regimes.

This paper is organized as follows. The model is described in Section II. In Section III, we present the numerical results. Section IV contains a summary and the conclusions.

## II. MODEL

We consider a cylindrically symmetric structure, whose active region (consisting of several quantum wells) is modeled as a single effective quantum well (QW) of radius  $a$  and thickness  $d_{\text{qw}}$ . Barrier regions of thickness  $d_b$  limit the QW region. Two highly reflecting mirrors separated by a distance  $L$  along the longitudinal  $z$  axis define the laser cavity. The injected current is  $I(r, t) = I_o$  for  $r < a$  and  $I(r, t) = 0$  otherwise.

The optical mode profile is determined by the built-in index guiding introduced by transverse refractive index step in the surrounding region. The core (cladding) refractive index is taken to be  $n_{\text{core}}$  ( $n_{\text{clad}}$ ), i.e., the transverse refractive index profile is  $n(r) = n_{\text{core}}$  for  $r < a$  and  $n(r) = n_{\text{clad}}$  for  $r > a$ .

Manuscript received February 23, 2003; revised August 13, 2003. This work was supported in part by the EPSRC, U.K., under Grant GR/R94404/01.

M. S. Torre is with the Instituto de Física “Arroyo Seco,” U.N.C.P.B.A, Pinto 399 (7000) Tandil, Argentina.

C. Masoller is with the Instituto de Física, Facultad de Ciencias, Universidad de la República, Montevideo 11400, Uruguay, and with the School of Informatics, University of Wales, Bangor LL57 1UT, Wales, U.K.

K. A. Shore is with the School of Informatics, University of Wales, Bangor LL57 1UT, Wales, U.K.

Digital Object Identifier 10.1109/JQE.2003.821484

By considering that due to its short cavity length the VCSEL supports a single longitudinal mode (but several transverse modes), the optical field can be split into longitudinal and transverse parts as

$$E(r, \theta, z, t) = \left[ \sum_{mn} \mathbf{E}_{mn}(r, \theta, t) \exp(i\omega_{mn}t) \right] f(z) \quad (1)$$

where  $\omega_{mn}$  is the angular oscillation frequency of the  $m$ th transverse mode of the free-running VCSEL and  $f(z)$  is determined by the round-trip condition in the plane wave approximation. For a Fabry–Perot cavity of length  $L$ ,  $f(z) = \sqrt{2L} \sin(p\pi z/L)$  with a  $p$  integer. For the circular transverse geometry of the VCSEL, the appropriate transverse modes are the linearly polarized LP $_{mn}$  modes [11], for which the transverse variation of the field is given by

$$\begin{aligned} \psi_{mn}(r, \theta) &= \frac{J_m(u_{mn}r/a)}{J_m(u_{mn})} \cos m\theta, \text{ for } r < a \\ \psi_{mn}(r, \theta) &= \frac{K_m(w_{mn}r/a)}{K_m(w_{mn})} \cos m\theta, \text{ for } r > a \end{aligned} \quad (2)$$

where  $J_m$  and  $K_m$  are Bessel functions of the first and second kinds, respectively,  $u_{mn} = a[(n_{\text{core}}k_{mn})^2 - \beta^2]^{1/2}$ ,  $w_{mn} = a[\beta^2 - (n_{\text{clad}}k_{mn})^2]^{1/2}$ ,  $\beta L = q\pi$ ,  $q$  is an integer, and the wavevector  $k_{mn}$  is obtained from eigenvalue equations.

To simplify the calculations, we consider two transverse modes that have azimuthal symmetry: the LP $_{01}$  and LP $_{02}$  modes

$$\psi_1(r) \equiv \psi_{01}(r, \theta)$$

and

$$\psi_2(r) \equiv \psi_{02}(r, \theta). \quad (3)$$

Their profiles are normalized such that  $\int_0^\infty |\psi_i(r)|^2 r dr = 1$ .

Since we are studying two transverse modes with parallel polarization, we have the scalar equation for the optical field

$$E(r, z, t) = [e_1(t)\psi_1(r) \exp(i\omega_1 t) + e_2(t)\psi_2(r) \exp(i\omega_2 t)]f(z) \quad (4)$$

where  $e_1(t)$  and  $e_2(t)$  are the slowly varying complex amplitudes of the transverse modes.  $\psi_i$  and  $f(z)$  are normalized such that  $|e_i|^2$  is proportional to the number of photons in the  $i$ th mode.

We assume a CW externally injected field of frequency  $\omega_{\text{inj}}$  that has an arbitrary transverse profile, which can be decomposed in terms of the LP $_{m,n}$  modes of the VCSEL.

The equations for the slowly varying complex amplitude of the transverse modes  $e_1(t)$ ,  $e_2(t)$ , the density of (confined) carriers in the QW regio,  $n_w(r, t)$ , and the density of (unconfined) carriers in the barrier regio,  $n_b(r, t)$  are [12]–[15]

$$\begin{aligned} \frac{de_1}{dt} &= \frac{1 + j\alpha}{2} \left( g_1 - \frac{1}{\tau_{p,1}} \right) e_1 \\ &+ \frac{\sqrt{P_{\text{inj},1}}}{\tau_{\text{in}}} \exp(j\Delta\omega_1 t) \end{aligned} \quad (5)$$

$$\begin{aligned} \frac{de_2}{dt} &= \frac{1 + j\alpha}{2} \left( g_2 - \frac{1}{\tau_{p,2}} \right) e_2 \\ &+ \frac{\sqrt{P_{\text{inj},2}}}{\tau_{\text{in}}} \exp(j\Delta\omega_2 t) \end{aligned} \quad (6)$$

$$\begin{aligned} \frac{\partial n_b}{\partial t} &= \frac{I_o}{ed_b\pi a^2} - \frac{n_b}{\tau_{\text{cap}}} + \frac{V_{\text{qw}} n_w}{V_b \tau_{\text{esc}}} \\ &- \frac{n_b}{\tau_n} + D_b \frac{1}{r} \frac{\partial}{\partial r} \left( r \frac{\partial n_b}{\partial r} \right) \end{aligned} \quad (7)$$

$$\begin{aligned} \frac{\partial n_w}{\partial t} &= \frac{V_b n_b}{V_{\text{qw}} \tau_{\text{cap}}} - \frac{n_w}{\tau_{\text{esc}}} - \frac{n_w}{\tau_n} - g_o(n_w - n_t)[|e_1|^2 |\psi_1|^2 \\ &+ |e_2|^2 |\psi_2|^2] + D_w \frac{1}{r} \frac{\partial}{\partial r} \left( r \frac{\partial n_w}{\partial r} \right). \end{aligned} \quad (8)$$

The first term on the right-hand side of (5) and (6) accounts for optical gain, losses, and phase-amplitude coupling. Here,  $\alpha$  is the linewidth enhancement factor and  $g_i$  is the modal gain, given as follows:

$$g_i(t) = \int_0^\infty g_o \Gamma_i(n_w - n_t) |\psi_i|^2 r dr \quad (9)$$

where  $g_o$  is the linear gain coefficient,  $\Gamma_i$  is the confinement factor for the  $i$ th mode, and  $n_t$  is the transparency carrier density.  $\tau_{p,i}$  is the photon lifetime for the  $i$ th mode.

The second term on the right-hand-side of (5) and (6) takes into account optical injection. The external field injects photons into the  $i$ th transverse mode with an efficiency that depends on the overlap of the transverse profiles of the injected field and the  $i$ th mode. This is taken into account through the modal injection strength  $P_{\text{inj},i}$ , which is proportional to the number of photons injected into the  $i$ th mode. The interaction of the injected field with the  $i$ th mode also depends on the frequency difference  $\Delta\omega_i = \omega_{\text{inj}} - \omega_i$ , which is the detuning of the injected field with respect to the  $i$ th mode frequency. In the rate-equation approach, the injection term has to be divided by the factor  $\tau_{\text{in}}$ , which is the VCSEL cavity round-trip time.

The terms on the right-hand side of (7) correspond, from left to right, to: 1) the rate at which carriers are injected into the barrier region; 2) the rate at which carriers are captured into the QWs; 3) the rate at which carriers escape out of the QWs; 4) the carrier loss owing to various nonradiative recombination processes; and 5) the last term accounts for carrier diffusion across the barrier region. The transport effects are included by a capture time  $\tau_{\text{cap}}$ , a escape time  $\tau_{\text{esc}}$ , and a diffusion coefficient  $D_b$ . The carrier loss is included by a carrier lifetime  $\tau_n$ . Since the variables  $n_b$  and  $n_w$  refer to carrier densities, the different sizes of the barrier and QW regions must be taken into account. This is done by the ratio  $V_b/V_{\text{qw}}$ , where  $V_b = d_b\pi a^2$  is the volume of the barrier region and  $V_{\text{qw}} = d_{\text{qw}}\pi a^2$  is the volume of the QW region.

The terms on the right-hand side of (8) correspond, from left to right, to: 1) the carriers captured into the QWs; 2) the carriers that escape out of the QWs; 3) the nonradiative carrier loss; 4) the carrier loss owing to stimulated recombination; and 5) the final term to carrier diffusion across the QWs.

### III. RESULTS

We solve numerically the model equations with the parameters given in Table I. The time integration step is  $\Delta t = 10^{-4}$  ps and the space integration step is  $\Delta r = 0.02 \mu\text{m}$ . The initial conditions used all through the paper correspond to the laser in the OFF state. The modal injection strength  $P_{\text{inj},i}$  and the frequency of the injected field  $\omega_{\text{inj}}$  are the free parameters of our

TABLE I  
PARAMETERS USED IN SIMULATIONS

Length of the VCSEL cavity $L$	$2 \mu\text{m}$
Solitary laser round-trip time $\tau_{\text{in}}$	$0.045 \text{ ps}$
Radius of the index-guiding region $a$	$6 \mu\text{m}$
Active region thickness $d_{wq}$	$0.024 \mu\text{m}$
Barrier region thickness $d_b$	$1.2 \mu\text{m}$
Refractive indices $n_{\text{core}}, n_{\text{clad}}$	3.4, 3.5
Linewidth enhancement factor $\alpha$	3
Linear gain coefficient $g_o$	$4.25 \times 10^{-9} \mu\text{m}^3/\text{ns}$
Carrier density at transparency $n_t$	$1.33 \times 10^6 \mu\text{m}^{-3}$
Capture and escape time $\tau_{\text{cap}}, \tau_{\text{esc}}$	5 ps, 25.5 ps
Carrier lifetime $\tau_n$	1.52 ns
Diffusion coefficients $D_w, D_b$	$0.5 \mu\text{m}^2/\text{ns}$
Confinement factors $\Gamma_1, \Gamma_2$	0.038
Photon lifetimes $\tau_{p,1}, \tau_{p,2}$	2.2 ps
Frequency difference between the modes $\omega_2 - \omega_1$	45 GHz

study. We consider two different values of the injection current: one such that in the absence of optical injection the LP<sub>01</sub> mode dominates ( $I_o = 2 \text{ mA}$ ), and one such that in the absence of optical injection both modes have nearly equal power ( $I_o = 3.2 \text{ mA}$ ).

In edge-emitting single-mode lasers, the injection strength has commonly been measured relative to the free-running modal power  $P_{\text{inj}} = K^2 P_{\text{sol}}$ , and typical values for the region of weak (large) injection are  $K < 0.01$  ( $K \gg 0.1$ ) [21]. Since in the model rate equations the relevant parameter is  $\sqrt{P_{\text{inj}}}/\tau_{\text{in}} = K\sqrt{P_{\text{sol}}}/\tau_{\text{in}}$ , due to the small value of  $\tau_{\text{in}}$  in VCSELS the injection regions shift to lower values of  $K$  (the locking region of a single-mode VCSEL for typical parameters and zero detuning occurs for  $K > 5 \times 10^{-3}$ , see [9, Fig. 1]). Since in multimode VCSELS the free-running modal powers are different, we measure the injection strength of the  $i$ th mode  $P_{\text{inj},i}$  relative to the free-running modal power  $P_{0,i}$ . We therefore define the parameter  $K_i$  as

$$P_{\text{inj},i} = K_i^2 P_{0,i}. \quad (10)$$

Let us first consider the situation in which the fundamental mode dominates ( $I_o = 2 \text{ mA}$ ). Fig. 1 displays the maximum, minimum, and average values of the oscillations of the modal intensities  $I_1(t) = |e_1(t)|^2$  and  $I_2(t) = |e_2(t)|^2$  as the strength of the injected field increases. The frequency of the injected field is tuned to match that of the dominant mode ( $\omega_{\text{inj}} = \omega_1$ ) and both modes are injected equally ( $P_{\text{inj},1} = P_{\text{inj},2} = P_{\text{inj}}$ ). The effect of asymmetric injection will be discussed later. Since the free-running modal powers are different, the injection ratio of the depressed mode  $K_2^2 = P_{\text{inj}}/P_{0,2}$  is larger than that of the dominant mode  $K_1^2 = P_{\text{inj}}/P_{0,1}$ . If the injection is weak enough, there are modal intensity oscillations (since the maximum and minimum values differ), while for stronger injection the modal intensities are constant and increase linearly with the injection strength.

Fig. 2 displays the maximum, minimum, and average values of the oscillations of the modal intensities when only the fundamental mode is coupled to the injected field ( $P_{\text{inj},2} = 0, P_{\text{inj},1} = P_{\text{inj}}$ ). In this case, we observe that the

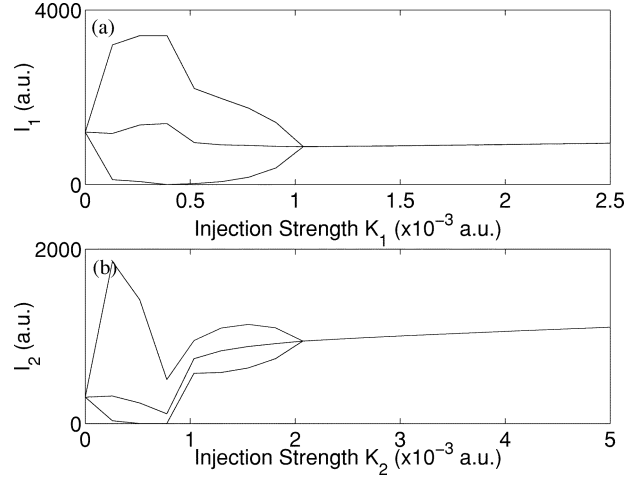


Fig. 1. Effect of increasing the injection strength when the LP<sub>01</sub> mode dominates ( $I_o = 2 \text{ mA}$ ).  $\omega_{\text{inj}} = \omega_1$ . Both modes are injected with the same number of photons ( $P_{\text{inj},1} = P_{\text{inj},2} = P_{\text{inj}}$ ). The relative injection rates  $K_1^2 = P_{\text{inj}}/P_{0,1}$  and  $K_2^2 = P_{\text{inj}}/P_{0,2}$  differ because the free-running modal powers are different (for  $I_o = 2 \text{ mA}$ ,  $P_{0,1} = 1200 \text{ a.u.}$  while  $P_{0,2} = 300 \text{ a.u.}$ ). We plot the maximum, minimum, and average values of (a)  $I_1(t)$  and (b)  $I_2(t)$ .

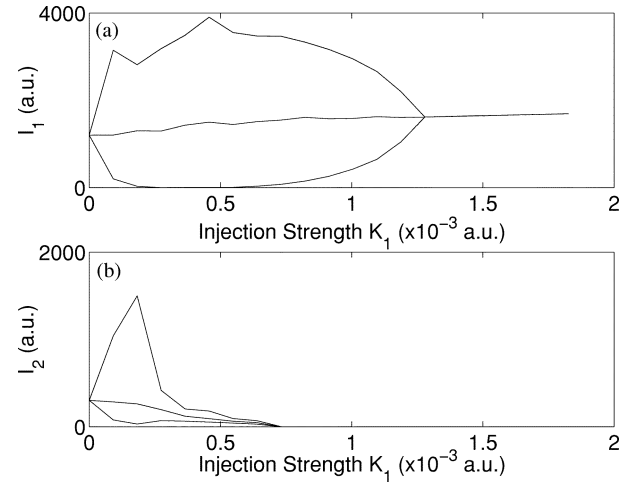


Fig. 2. Effect of increasing the injection strength when only the LP<sub>01</sub> mode interacts with the injected field ( $P_{\text{inj},2} = 0, P_{\text{inj},1} = P_{\text{inj}}$ ).  $I_o = 2 \text{ mA}$ ,  $\omega_{\text{inj}} = \omega_1$ . We plot the maximum, minimum, and average values of (a)  $I_1(t)$  and (b)  $I_2(t)$ .

LP<sub>02</sub> mode is rapidly suppressed as the injection increases. However, the injection locking regime occurs for higher injection strength with respect to that when both modes are coupled to the injected field.

Similar results are observed in the operating regime where both modes are equally dominant ( $I_o = 3.2 \text{ mA}$ ). Figs. 3 and 4 display results when both modes interact equally with the injected field and when only the fundamental mode interacts with the injected field, respectively. For weak injection, there are oscillations in the intensities of the two modes, and above a certain injection level we observe steady-state dynamics. The intensities of both modes grow steadily with the injection strength. On the contrary, if the modes have orthogonal polarizations and the injected field interferes only with one of them, we observe that strong enough injection depresses (and eventually completely suppresses) the other mode. Notice, however, that when

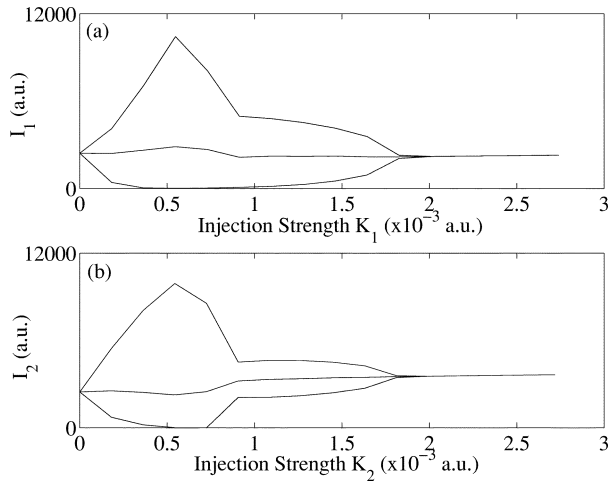


Fig. 3. Maximum, minimum, and average values of the intensity (a) of the  $LP_{01}$  mode and (b) of intensity of the  $LP_{02}$  mode as a function of the injection coefficient when  $P_{inj,1} = P_{inj,2}$ ,  $\omega_{inj} = \omega_1$ ,  $I_0 = 3.2$  mA.

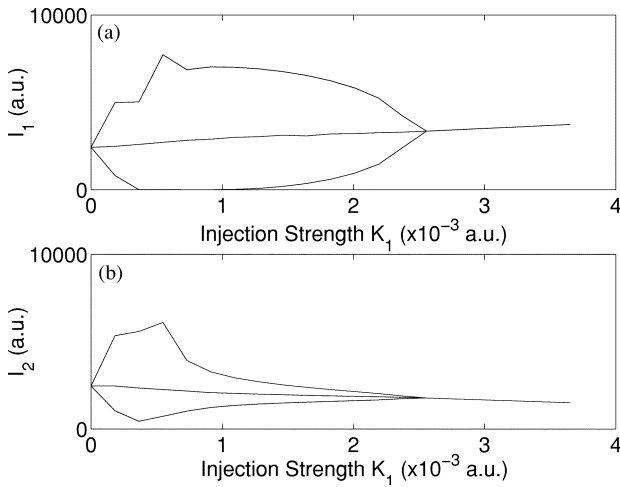


Fig. 4. Maximum, minimum, and average values of the intensity (a) of the  $LP_{01}$  mode and (b) of intensity of the  $LP_{02}$  mode as a function of the injection coefficient when  $P_{inj,1} = P_{inj}$  and  $P_{inj,2} = 0$ ,  $\omega_{inj} = \omega_1$ ,  $I_0 = 3.2$  mA.

the field interacts only with the  $LP_{01}$  mode injection locking begins at higher injection strengths than when it interacts with both modes.

In the region where the modal intensities reach a constant value, the optical spectrum reveals that the frequencies of both transverse modes lock to that of the injected field. As could be expected, a rich variety of complex nonlinear behaviors occurs outside the injection locking region. In agreement with the experimental observations of Hong *et al.* [10], we found parameter regions where the frequency of one mode locks to that of the injected field, while the frequency of the other mode remains unperturbed [Fig. 5(a) and (c)]. In these regions the modal intensities oscillate inphase [Fig. 5(b) and (d)] at the frequency  $\omega_2 - \omega_1$  (where  $\omega_i$  is the frequency of the  $i$ th mode with injection). The mode whose frequency differs from that of the injected field exhibits the larger oscillations.

There are also parameter regions where none of the frequencies of the modes lock to that of the injected field, and new frequencies appear in the optical spectrum [Fig. 6(a), (c), and (e)].

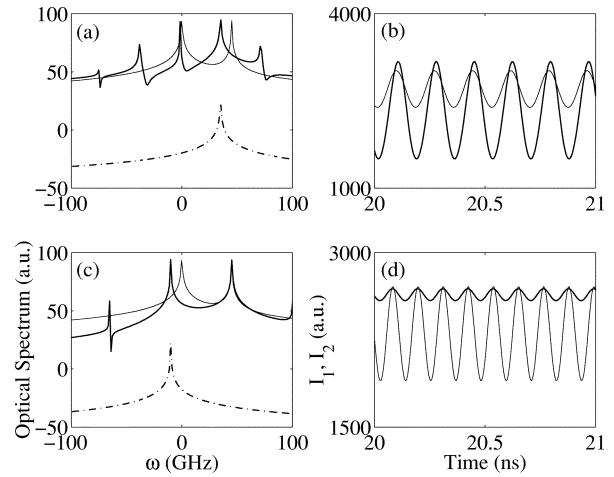


Fig. 5. Optical spectrum and time evolution of the modal intensities. We plot the spectrum of the laser field with optical injection (thick solid line), of the free-running laser (thin solid line), and of the injected field (dot-dashed line). The zero of the horizontal axis coincides with  $\omega_1$  (and, thus, the frequency of the  $LP_{02}$  mode of the free-running laser is  $\omega_2 = 45$  GHz). We plot the power of the fundamental mode with a thick line and the power of the  $LP_{02}$  mode with a thin line. (a), (b)  $I_0 = 3.2$  mA,  $K_1 \sim K_2 \sim 1.8 \times 10^{-4}$ . (c)  $\omega_{inj} - \omega_1 = 35$  GHz. (d)  $\omega_{inj} - \omega_1 = -10$  GHz.

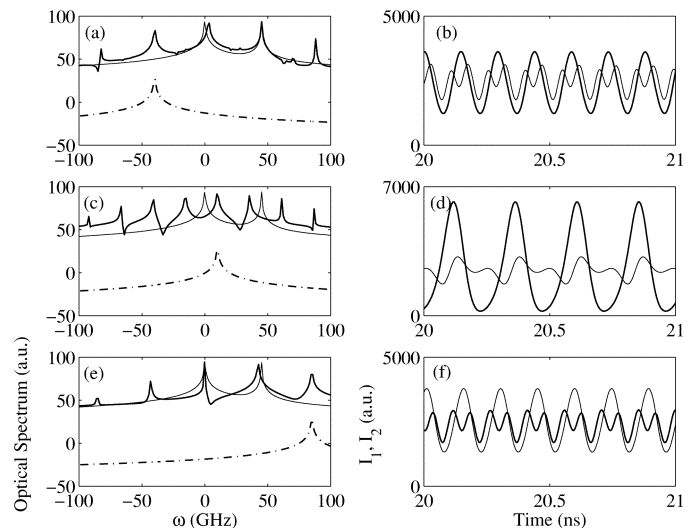


Fig. 6. Optical spectrum and time evolution of the modal intensities. We plot the spectrum of the laser field with optical injection (thick solid line), of the free-running laser (thin solid line), and of the injected field (dot-dashed line). The zero of the horizontal axis coincides with  $\omega_1$  (and, thus, the frequency of the  $LP_{02}$  mode of the free-running laser is  $\omega_2 = 45$  GHz). We plot the power of the fundamental mode with a thick line and the power of the  $LP_{02}$  mode with a thin line. (a), (b)  $I_0 = 3.2$  mA,  $K_1 \sim K_2 \sim 3.6 \times 10^{-4}$ . (c)  $\omega_{inj} - \omega_1 = -40$  GHz. (d)  $\omega_{inj} - \omega_1 = 10$  GHz. (e), (f)  $\omega_{inj} - \omega_1 = 80$  GHz.

In these regions, there is a dynamic behavior where the modal intensities oscillate partially inphase and partially out of phase [Fig. 6(b), (d), and (f)]. Chaotic pulsing behavior has also been observed [Fig. 7(a) and (b)]. In tiny parameter regions (for weak injection and  $\omega_{inj} = (\omega_2 - \omega_1)/2$ ), there is complete antiphase behavior [Fig. 7(c) and (d)].

Since the coupling of the injected field with a transverse mode depends on the overlap of their spatial profiles, the coupling of the injected field with the fundamental and the  $LP_{02}$  modes will in general be different. Therefore, the parameters  $P_{inj,1}$  and  $P_{inj,2}$ , which measure the number of photons injected into the

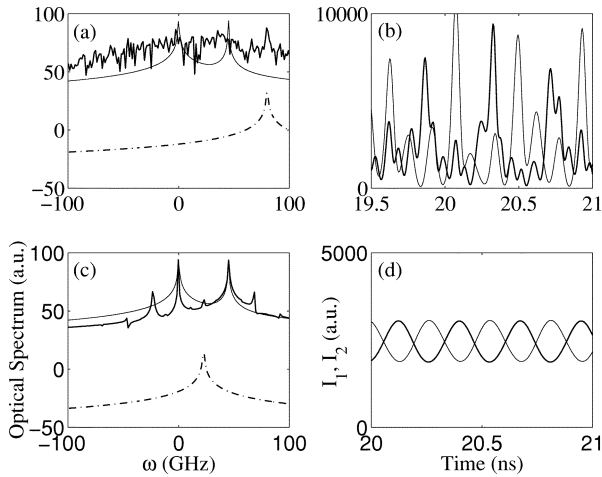


Fig. 7. Optical spectrum and time evolution of the modal intensities. We plot the spectrum of the laser field with optical injection (thick solid line), of the free-running laser (thin solid line), and of the injected field (dot-dashed line). The zero of the horizontal axis coincides with  $\omega_1$  (and, thus, the frequency of the LP<sub>02</sub> mode of the free-running laser is  $\omega_2 = 45$  GHz). We plot the power of the fundamental mode with a thick line and the power of the LP<sub>02</sub> mode with a thin line.  $I_0 = 3.2$  mA. (a), (b)  $K_1 \sim K_2 \sim 7.3 \times 10^{-4}$ ,  $\omega_{inj} - \omega_1 = 80$  GHz. (c), (d)  $K_1 \sim K_2 \sim 9 \times 10^{-5}$ ,  $\omega_{inj} - \omega_1 = 22.5$  GHz.

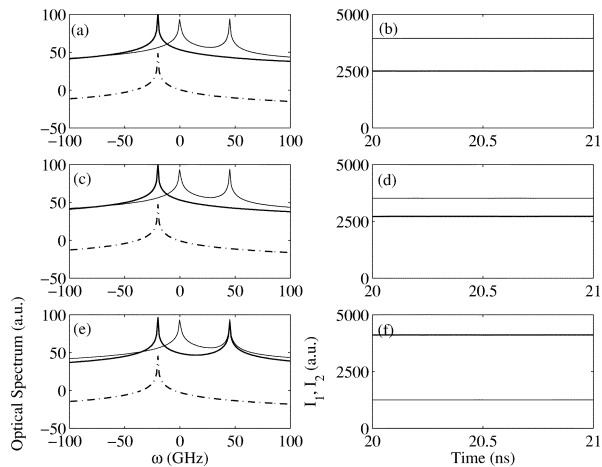


Fig. 8. Optical spectrum and time evolution of the modal intensities. We plot the spectrum of the laser field with optical injection (thick solid line), of the free-running laser (thin solid line), and of the injected field (dot-dashed line). The zero of the horizontal axis coincides with  $\omega_1$  (and, thus, the frequency of the LP<sub>02</sub> mode of the free-running laser is  $\omega_2 = 45$  GHz). We plot the power of the fundamental mode with a thick line and the power of the LP<sub>02</sub> mode with a thin line.  $I_0 = 3.2$  mA,  $\omega_{inj} - \omega_1 = -10$  GHz. (a)  $K_1 \sim 0.0036$ . (b)  $K_2 = K_1$ . (c), (d)  $K_2 = K_1/4$ . (e), (f)  $K_2 = 0$ .

LP<sub>01</sub> and LP<sub>02</sub> modes, will in general be different. Nevertheless, we find that the regimes discussed previously for symmetric coupling ( $P_{inj,1} = P_{inj,2}$ ) also occur when  $P_{inj,1}$  and  $P_{inj,2}$  differ. As an example, Fig. 8 displays results for injection locking when  $P_{inj,2} = P_{inj,1}$  [Fig. 8 (a) and (b)];  $P_{inj,2} = P_{inj,1}/2$  [Fig. 8 (c) and (d)] and  $P_{inj,2} = 0$  [Fig. 8(e) and (f)]. When both modes receive strong enough injection, their frequencies lock to that of the injected field [Fig. 8(a) and (c)]. We point out that the modal powers vary with the number of injected photons [note that the value of  $I_2$  in Fig. 8(d) is lower than in Fig. 8(b)]. When the LP<sub>02</sub> mode is not coupled to the injected field, its frequency remains unperturbed as only the frequency of the injected mode locks to that of the injected field [Fig. 8(e)].

#### IV. CONCLUSION

We have studied numerically the behavior of a VCSEL having two transverse modes with parallel polarization, which interact with an externally injected CW optical field. We used a model that includes spatial profiles for the two transverse modes and for two types of carriers, those in the QW and those in the barrier regions of the VCSEL. The model applies to weakly index-guided VCSELS, where the transverse modal profiles and the free-running modal frequencies are determined by the built-in refraction index distribution, thus allowing a description in terms of modal amplitudes. The externally injected field was assumed to have an arbitrary transverse profile, which was decomposed in terms of the transverse modes of the VCSEL.

In agreement with the experimental results of [10], we found that it is not possible to induce single-transverse-mode behavior by optical injection when the injected field interacts with the two transverse modes. Different dynamic regimes were found depending on the injection strength and frequency of the injected field. Strong enough injection induces a two-mode injection locking regime, where the frequencies of both transverse modes lock to that of the injected field. Weak injection induces different behaviors including in-phase mode oscillations, mixed states where inphase and out of phase oscillations alternate, antiphase oscillations, and chaotic pulsing.

It is well known that optically injected semiconductor lasers exhibit complex nonlinear behavior. We have shown that, when the injected field interacts with more than one transverse mode, an even richer dynamics arises. It will be interesting in the future to study the dynamics when the injected field interacts with an arbitrary number of transverse modes with parallel and orthogonal polarizations.

#### ACKNOWLEDGMENT

The authors would like to thank Y. Hong for useful discussion.

#### REFERENCES

- [1] Z. G. Pan, S. J. Jiang, M. Dagenais, R. A. Morgan, K. Kojima, M. T. Asom, R. E. Leibenguth, G. D. Guth, and M. W. Focht, "Optical-injection induced polarization bistability in vertical-cavity surface-emitting lasers," *Appl. Phys. Lett.*, vol. 63, pp. 2999–3001, 1993.
- [2] H. Li, T. L. Lucas, J. G. McInerney, M. W. Wright, and R. A. Morgan, "Injection locking dynamics of vertical cavity semiconductor lasers under conventional and phase conjugate injection," *IEEE J. Quantum Electron.*, vol. 32, pp. 227–235, 1996.
- [3] D. L. Boiko, G. M. Stephan, and P. Besnard, "Fast polarization switching with memory effect in a vertical cavity surface emitting laser subject to modulated optical injection," *J. Appl. Phys.*, vol. 86, pp. 4096–4099, 1999.
- [4] K. Panajotov, F. Berghmans, M. Peeters, G. Verschaffelt, J. Danckaert, I. Veretennicoff, and H. Thienpont, "Data transparent reconfigurable optical interconnections using polarization switching in VCSEL's induced by optical injection," *IEEE Photon. Technol. Lett.*, vol. 11, pp. 985–987, 1999.
- [5] B. Lucke, G. Hergenhan, U. Brauch, and A. Giesen, "Phase tuning of injection-locked VCSELS," *IEEE Photon. Technol. Lett.*, vol. 13, pp. 100–102, 2001.
- [6] C. H. Chang, L. Chrostowski, C. J. Chang-Hasnain, and W. W. Chow, "Study of long-wavelength VCSEL-VCSEL injection locking for 2.5-Gb/s transmission," *IEEE Photon. Technol. Lett.*, vol. 14, pp. 1635–1637, 2002.

- [7] S. Bandyopadhyay, Y. Hong, P. S. Spencer, and K. A. Shore, "Experimental observation of anti-phase polarization dynamics in VCSELS," *Opt. Commun.*, vol. 202, pp. 145–154, 2002.
- [8] Y. Hong, P. S. Spencer, S. Bandyopadhyay, P. Rees, and K. A. Shore, "Polarization-resolved chaos and instabilities in a vertical cavity surface emitting laser subject to optical injection," *Opt. Commun.*, vol. 216, pp. 185–190, 2003.
- [9] J. Y. Law, G. H. M. van Tartwijk, and G. P. Agrawal, "Effects of transverse-mode competition on the injection dynamics of vertical-cavity surface-emitting lasers," *Quantum Semiclass. Opt.*, vol. 9, pp. 737–747, 1997.
- [10] Y. Hong, P. S. Spencer, P. Rees, and K. A. Shore, "Optical injection dynamics of two-mode vertical cavity surface-emitting semiconductor lasers," *IEEE J. Quantum Electron.*, vol. 38, pp. 274–278, 2002.
- [11] M. S. Sodha and A. K. Ghatak, *Inhomogeneous Optical Waveguides*. New York: Plenum, 1977.
- [12] A. Valle, J. Sarma, and K. A. Shore, "Dynamics of transverse-mode competition in vertical-cavity surface-emitting laser-diodes," *Opt. Commun.*, vol. 115, pp. 297–302, 1995.
- [13] —, "Spatial holeburning effects on the dynamics of vertical-cavity surface-emitting laser-diodes," *IEEE J. Quantum Electron.*, vol. 31, pp. 1423–1431, 1995.
- [14] W. Rideout, W. F. Sharfin, E. S. Koteles, M. O. Vassell, and B. Elman, "Well-barrier hole burning in quantum-well lasers," *IEEE Photon. Technol. Lett.*, vol. 3, pp. 784–786, 1991.
- [15] R. Nagarajan, T. Fukushima, S. W. Corzine, and J. E. Bowers, "Effects of carrier transport on high-speed quantum-well lasers," *Appl. Phys. Lett.*, vol. 59, pp. 1835–1837, 1991.
- [16] G. H. M. van Tartwijk and D. Lenstra, "Semiconductor lasers with optical injection and feedback," *Quantum Semiclass. Opt.*, vol. 7, pp. 87–143, 1995.
- [17] J. Sacher, D. Baums, P. Pankin, W. Elsaesser, and E. O. Goebel, "Intensity instabilities of semiconductor lasers under current modulation, external light injection, and delayed feedback," *Phys. Rev. A*, vol. 45, pp. 1893–1905, 1992.
- [18] V. Annovazzi-Lodi, S. Donati, and M. Manna, "Chaos and locking in a semiconductor laser due to external injection," *IEEE J. Quantum Electron.*, vol. 30, pp. 1537–1541, 1994.
- [19] V. Kovanis, A. Gavrielides, T. B. Simpson, and J. M. Liu, "Instabilities and chaos in optically injected semiconductor lasers," *Appl. Phys. Lett.*, vol. 67, pp. 2780–2782, 1995.
- [20] A. Gavrielides, V. Kovanis, P. M. Varangis, T. Erneux, and G. Lythe, "Coexisting periodic attractors in injection-locked diode lasers," *Quantum Semiclass. Opt.*, vol. 9, pp. 785–796, 1997.
- [21] V. Annovazzi-Lodi, A. Scire, M. Sorel, and S. Donati, "Dynamic behavior and locking of a semiconductor laser subjected to external injection," *IEEE J. Quantum Electron.*, vol. 34, pp. 2350–2357, 1998.
- [22] S. Wieczorek, B. Krauskopf, and D. Lenstra, "Mechanisms for multistability in a semiconductor laser with optical injection," *Opt. Commun.*, vol. 183, pp. 215–226, 2000.
- [23] M. G. Zimmermann, M. A. Natiello, and H. G. Solari, "Global bifurcations in a laser with injected signal: Beyond Adlers approximation," *Chaos*, vol. 11, pp. 500–513, 2001.
- [24] S. Wieczorek, B. Krauskopf, and D. Lenstra, "Multipulse excitability in a semiconductor laser with optical injection," *Phys. Rev. Lett.*, vol. 88, pp. 063 901-1–063 901-4, 2002.
- [25] S. Wieczorek, T. B. Simpson, B. Krauskopf, and D. Lenstra, "Bifurcation transitions in an optically injected diode laser: Theory and experiment," *Opt. Commun.*, vol. 215, pp. 125–134, 2003.

**M. S. Torre** received the Licenciada en Física (Ms.Sc.) degree and the Ph.D. degree both from the Universidad Nacional del Centro de la Provincia de Buenos Aires (UNCPBA), Buenos Aires, Argentina.

Her research was primarily in external driven laser physics. From 1995 to 1997, she was a Post-Doctoral Fellow at the Photonics Technology Department of the ETSI Telecomunicaciones, Universidad Politécnica de Madrid, Madrid, Spain. Her research was in quantum-well semiconductor laser modeling. Since 1988, she has been member of the Quantum Electronic Group of the Physics Institute "Arroyo Seco," UNCPBA. She is currently a Research Professor at the Facultad de Ciencias Exactas of the UNCPBA. Her research topics include modeling and dynamics of VCSEL, dynamics of semiconductor lasers with external optical feedback, and diffusion effects in semiconductor lasers.

**Cristina Masoller** Masoller was born in Montevideo, Uruguay, in 1963. She received the M.Sc. degree in physics from the Universidad de la Republica, Montevideo, Uruguay, in 1991 and the Ph.D. degree in physics from Bryn Mawr College, Bryn Mawr, PA, in 1999.

She was a Visiting Professor at the Physics Department, Universitat de les Illes Balears, Spain (September–October 2001, February–March 2002, and September 2002) and Visiting Researcher at the School of Informatics, University of Wales, Bangor, U.K. (October 2002–January 2003 and October–November 2003). Since 1993, she has been with the Physics Department of the School of Sciences, Universidad de la Republica, where she is an Associate Professor. In 2003, she became a Regular Associate of the Abdus Salam International Centre for Theoretical Physics, Trieste, Italy. She has authored or coauthored over 40 journal papers. Her research interests include theoretical modeling of chaotic systems, synchronization and stochastic phenomena, nonlinear dynamics of semiconductor lasers, and time-delayed systems.

**K. A. Shore** received the degree in mathematics from the University of Oxford, Oxford, U.K., and the Ph.D. degree from University College, Cardiff, Wales, U.K. His doctoral work was concerned with the electrical and optical properties of double-heterostructure semiconductor lasers.

He was a Lecturer at the University of Liverpool, Liverpool, U.K. (1979–1983) and then at the University of Bath, Bath, U.K., where he became Senior Lecturer (1986), Reader (1990), and Professor (1995). In 1995, he was appointed to the Chair of Electronic Engineering, University of Wales, Bangor, Wales, U.K., where he is currently the Head of the School of Informatics. He is the Director of Industrial and Commercial Optoelectronics (ICON), a Welsh Development Agency Centre of Excellence which has a mission to "make light work" through the utilization of Bangor optoelectronics expertise and facilities. He is also a member of the steering committee of the Welsh Optoelectronics Forum. His research work has been principally in the area of semiconductor optoelectronic device design and experimental characterization with particular emphasis on nonlinearities in laser diodes and semiconductor optical waveguides. He has authored or coauthored over 600 contributions to archival journals, books, and technical conferences. He was a visiting researcher at the Center for High Technology Materials, University of New Mexico, Albuquerque, in 1987. He received a Royal Society Travel Grant to visit universities and laboratories in Japan in July 1988. In 1989, he was a Visiting Researcher at the Huygens Laboratory, Leiden University, The Netherlands. During the summers of 1990 and 1991, he worked at the Teledanmark Research Laboratory and the MIDIT Center of the Technical University of Denmark, Lyngby. He was a guest researcher at the Electrotechnical Laboratory (ETL), Tsukuba, Japan, in 1991. In 1992, he was a Visiting Professor at the Department of Physics, University de les Illes Balears, Palma-Mallorca, Spain. He was a Visiting Lecturer with the Instituto de Fisica de Cantabria, Santander, Spain, in June 1996 and 1998 and a Visiting Researcher in the Centre for Laser Applications, Department of Physics, Macquarie University, Sydney, Australia, in July/August 1996, 1998, and 2000 and April 2002. In July/August 2001, he was a Visiting Researcher at the ATR Adaptive Communications Laboratories, Kyoto, Japan. His current research interests include multiwave mixing and optical switching in semiconductor lasers, design and fabrication of intersubband semiconductor lasers and organic semiconductor lasers, dynamics of vertical-cavity semiconductor lasers, and applications of nonlinear dynamics in semiconductor lasers to optical data encryption.

Dr. Shore, cofounded and acts as Organizer and Programme Committee Chair for the international conference on Semiconductor and Integrated Optoelectronics (SIOE) which, since 1987, has been held annually in Cardiff, Wales, U.K. He was Programme Chair for the UK National Quantum Electronic Conference (QE'13) and was European Liaison Committee chair for the OSA Integrated Photonics Research (IPR'98) conference in Victoria, BC, Canada, in 1998. He was a member of the programme committee for IPR'99 Santa Barbara, CA, in July 1999 and also the European Conference on Integrated Optics (ECIO), Torino, Italy, in April 1999. He is a coorganizer of a Rank Prize Symposium on Nonlinear Dynamics in Lasers held in the Lake District, U.K., in August 2002. He was a technical committee member for CLEO (Europe) 2003.